

Review

A Ten-Year Perspective on Twist-Bend Nematic Materials

Richard J. Mandle ^{1,2} ¹ School of Physics and Astronomy, University of Leeds, Leeds LS2 9JT, UK; r.mandle@leeds.ac.uk² School of Chemistry, University of Leeds, Leeds LS2 9JT, UK

Abstract: The discovery of the twist-bend nematic phase (N_{TB}) is a milestone within the field of liquid crystals. The N_{TB} phase has a helical structure, with a repeat length of a few nanometres, and is therefore chiral, even when formed by achiral molecules. The discovery and rush to understand the rich physics of the N_{TB} phase has provided a fresh impetus to the design and characterisation of dimeric and oligomeric liquid crystalline materials. Now, ten years after the discovery of the N_{TB} phase, we review developments in this area, focusing on how molecular features relate to the incidence of this phase, noting the progression from simple symmetrical dimeric materials towards complex oligomers, non-covalently bonded supramolecular systems.

Keywords: liquid crystals; twist-bend nematic; liquid crystal dimers; nematic

1. Introduction

The term “liquid crystal” refers to a large number of states of matter that possess some degree of positional and/or orientational order, which is intermediate between isotropic liquids and crystalline solids. Much has been written about nematic liquid crystals and the twist-bend nematic phase, and so for the sake of brevity a short introduction to the topic suffices. The uniaxial nematic phase is arguably the simplest liquid crystal phase, with the constituent molecules (or particles) being, on average, oriented along a vector termed the director. Nematic liquid crystals are of special interest due to their role in display technology, and the discovery of new nematic ground states such as the twist-bend nematic is met with great enthusiasm. Biaxial nematics, in which the molecules are oriented along two orthogonal directors [1], are known to exist [2], but are outside the scope of this review. Similarly, although beyond the scope of this review, we note that nematic phases are almost exclusively *apolar*, that is, molecules orient both parallel and antiparallel to the director; very recently, the polar ferroelectric nematic phase has been shown to exist [3–7].

Introduction of chirality to a nematic liquid crystal leads to the formation of a chiral nematic phase, which has a helical superstructure. Dozov and Meyer independently suggested that bent shaped molecules could spontaneously form a heliconical nematic structure that is locally chiral, even when formed of achiral molecules [8]. This is termed the twist-bend nematic (N_{TB}) phase, and was reported experimentally in a landmark work in 2011 [9]. The N_{TB} phase has been described as the “structural link” between the uniaxial nematic phase and the helical chiral nematic mesophase [10]. A number of techniques have measured [10–13] (or inferred [14,15]) the repeat length of the N_{TB} phase, with in situ resonant X-ray scattering being particularly noteworthy [16,17], and while the precise pitch length is material dependent, a value of around 10 nm is typical. This being said, other models have been proposed that merit further experimental investigation [18], but were outside the scope of this review.

The average conical angle between the mesogens and the helical axis can be measured by NMR [19] or birefringence [20], or by reconstructing the ODF using order parameter data from, for example, SAXS [21], polarised Raman spectroscopy [22], or NMR [23]. The conical angle of the N_{TB} phase remains below the magic angle and the phase is uniaxial with positive birefringence, confirmed by conoscopic investigation [24]. Calorimetric studies



Citation: Mandle, R.J. A Ten-Year Perspective on Twist-Bend Nematic Materials. *Molecules* **2022**, *27*, 2689. <https://doi.org/10.3390/molecules27092689>

Academic Editor: Borislav Angelov

Received: 31 March 2022

Accepted: 20 April 2022

Published: 21 April 2022

Publisher's Note: MDPI stays neutral with regard to jurisdictional claims in published maps and institutional affiliations.



Copyright: © 2022 by the author. Licensee MDPI, Basel, Switzerland. This article is an open access article distributed under the terms and conditions of the Creative Commons Attribution (CC BY) license (<https://creativecommons.org/licenses/by/4.0/>).

show the N_{TB} -N is typically first order, and close to tricritical [9,25–28]. The N_{TB} phase has been shown to be strongly shear thinning; for the material KA(0.2), a 6-component mixture with a pitch length of 10.5 nm [29,30], it was shown that at low (<1 Pa) shear stress, the viscosity was $\sim 1000\times$ larger than the nematic phase. For the same material at high shear stress (>10 Pa), the viscosity of the N_{TB} -phase dropped by two orders of magnitude as the helix underwent shear-induced realignment [31].

As with all mesophases, the formation of the N_{TB} phase in a given material is intimately linked to molecular structure, and there has been significant effort in the design of new materials that exhibit the N_{TB} phase [32]. The molecular structure of liquid crystalline dimers can be subdivided into distinct regions, as outlined in Figure 1B. In the simplest terms, a dimer consists of two rigid mesogenic units joined by a flexible spacer [33–35]. For a trimer, three mesogenic units are joined in a similar fashion, and so on. Today, in the region of 1000, materials are known to exhibit the N_{TB} phase, and so in this review, we focused on systematic variations to key areas of molecular structure rather than making a futile attempt to cover all materials.

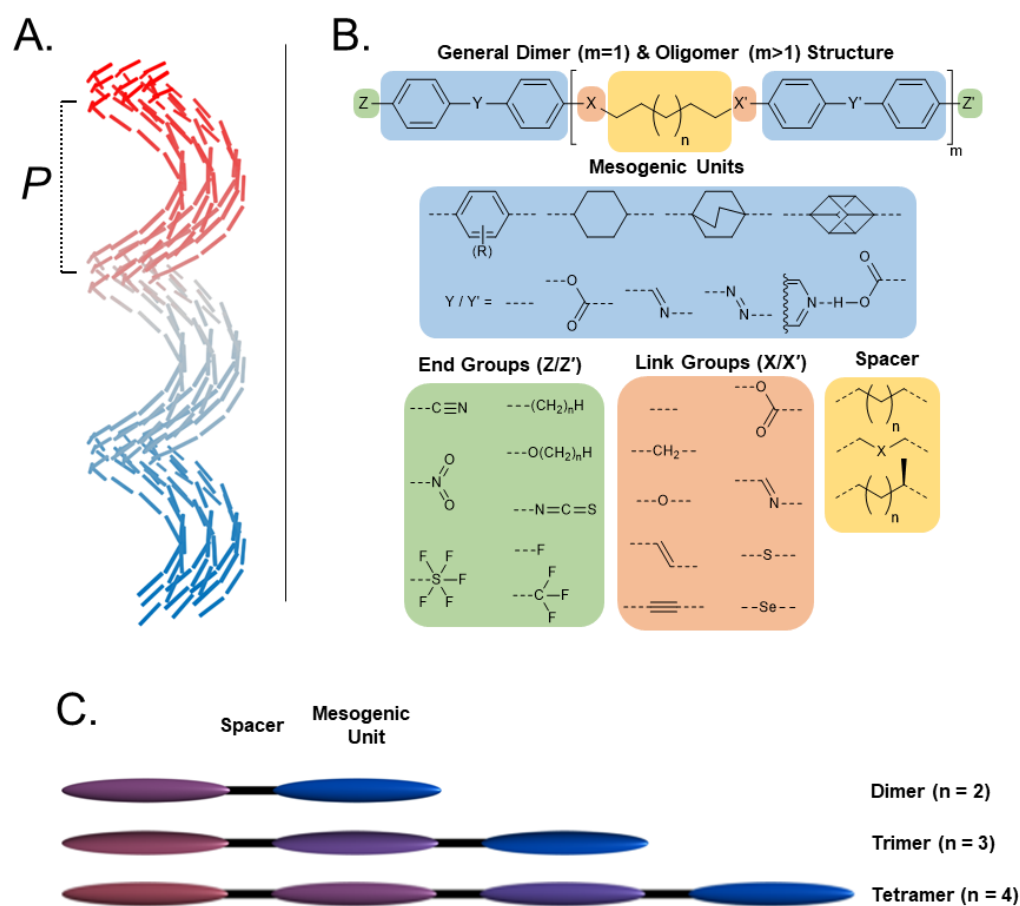


Figure 1. (A) Cartoon depiction of the helical director precession in the twist-bend nematic phase; mesogenic units are shown as cylinders, and are coloured according to their position along the helix axis. (B) The general structure of terminally appended liquid crystalline dimers and oligomers, subdivided into regions of interest to this review. For each subdivision example, chemical fragments that have been utilised in N_{TB} materials are given. (C) Schematic depiction of the relationship between dimers, trimers, and tetramers in terms of their subunit composition.

2. Materials

The CBnCB family are archetypal N_{TB} materials, and a logical place to begin our review. These materials feature two cyanobiphenyl mesogenic units separated by n methylene units. As with all LC dimers, the CBnCB family displays a strong odd–even effect, with the

even parity members displaying notably higher clearing points than those with odd spacer parity. With the exception of the shortest homologue (CB3CB), all odd parity CB n CBs displayed two nematic phases, the lower temperature nematic phase being identified as the N_{TB} phase (Table 1). Even parity CB n CB materials displayed only a conventional nematic phase.

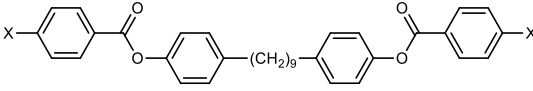
Table 1. Transition temperatures (T_{A-B}, °C) of the CB n CB family of materials [9,23,26,36–40].

No.	Name	<i>n</i>	T _{MP}	T _{N_{TB}-N}	T _{N-Iso}
1	CB3CB	3	142.1	-	-
2	CB5CB	5	150	92	97
3	CB6CB	6	183	-	230
4	CB7CB	7	102	104.5	116
5	CB8CB	8	175	-	195.9
6	CB9CB	9	83	105.0	119.8
7	CB10CB	10	140	-	174.1
8	CB11CB	11	99.9	108.6	125.5
9	CB12CB	12	139	-	157
10	CB13CB	13	106	105	122

Due to their favourable working temperatures, the properties of the N_{TB} phase of some members of the CB n CB family have been quite well explored. The helix pitch length of CB7CB was measured by freeze-fracture TEM by Chen et al. [11], who found a value of 8.3 nm. Later, Zhu et al. measured the N_{TB} pitch length of CB9CB as a function of temperature by resonant X-ray scattering at the carbon K-edge [16]; the pitch length was largest close to the N_{TB}-N transition (~9.8 nm), and decreased to around 8 nm with decreasing temperature. Yu and Wilson recently reported fully atomistic MD simulations of CB7CB, which yielded an N_{TB} phase with a pitch length of 8.35 nm [41]. The conical tilt-angle within these simulations (~29°) agreed well with the experimental values [11,20].

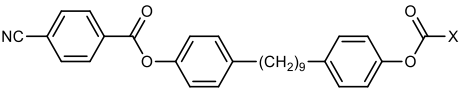
The orientational order parameters of several members of the CB n CB family have been measured, with results from different methods generally being consistent with one another. For odd parity CB n CBs, the thermal evolution of orientational order within the nematic phase is unremarkable, however, at T_{N_{TB}-N}, there is a decrease in orientational ordering. This decrease results from the molecules tilting away from the helix, which manifests as a reduction in, or even negative value of <P₄> [21,42]. This behaviour of the orientational order parameters has also been observed by NMR [43], and is reported to be consistent with the polar twisted nematic (N_{PT}) model of the N_{TB} phase. CB8CB, which has even spacer parity and does not show the N_{TB} phase, displays unusually large nematic order parameters [22], as does CB10CB [43].

We next consider variations in the mesogenic units. Compound 11 belongs to a class of materials known as “PZP” dimers (P = phenyl, Z = carboxylate ester). The synthesis of these materials is trivial; the penultimate step is esterification of *bis* 1,9-(4-hydroxyphenyl)nonane, permitting the synthesis of a large number of variations in core structure via esterification. In Table 2, we present the transition temperatures of a set of PZP-9-PZP dimers with varying terminal groups. While cyano, isothiocyanato, and alkyl/alkoxy groups are found to support the formation of the N_{TB} phase [44,45], various other polar units (nitro, fluoro, trifluoromethyl, pentafluorosulphanyl) render the resulting materials non-mesogenic [44]. For compound 15, the -NCS unit enables measurement of the N_{TB} pitch length (~9 nm) using resonant X-ray scattering at the carbon K-edge and also the sulphur K-edge [46].

Table 2. Transition temperatures (T_{A-B} , °C) of some symmetric (PZP)-9 materials with varying terminal unit [44,45].


No.	X	T_{MP}	$T_{N_{TB-N}}$	T_{N-Iso}
11	-CN	157.6	114.5	146.6
12	-NO ₂	105.4	-	-
13	-F	97.6	-	-
14	-CF ₃	102.4	-	-
15	-NCS	97.7	103.7	127.4
16	-SF ₅	123.0	-	-
17	-C ₅ H ₁₁	72.8	58.8	66.2
18	-OC ₅ H ₁₁	71.8	76.0	86.6

The synthetic flexibility afforded by the PZP dimers makes it possible to prepare dissymmetric materials such as those shown in Table 3 [47,48]. With a single phenyl 4-cyanobenzoate mesogenic unit, it is possible to obtain materials that display the N_{TB} phase, even when the second mesogenic unit incorporates an ‘unfavourable’ terminal unit (e.g., NO₂, SF₅, etc.) [47,48]. This approach also lends itself to the synthesis of trimers, tetramers, and so on, as will be discussed later. A general trend in the materials presented in Table 3 is that the addition of additional fluorine atoms *ortho* to the terminal group leads to depressions in both $T_{N_{TB-N}}$ and T_{N-Iso} , mirroring the behaviour of calamitic materials [49]. One advantage enjoyed by unsymmetrical materials is that their melting points are generally lower than those of the corresponding symmetrical derivatives, which compensates for the more elaborate synthesis required.

Table 3. Transition temperatures (T_{A-B} , °C) of some dissymmetric (PZP)-9 materials with varying terminal unit [47,48].


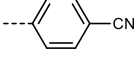
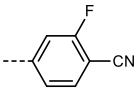
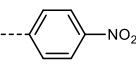
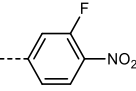
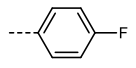
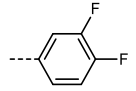
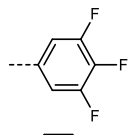
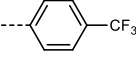
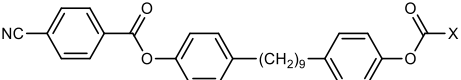
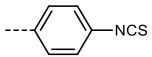
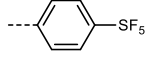
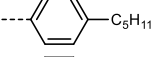
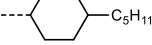
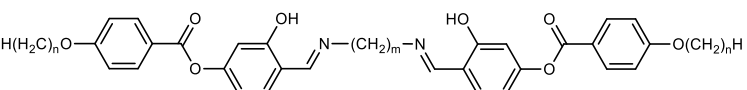
No.	X	T_{MP}	$T_{N_{TB-N}}$	T_{N-Iso}
11		157.6	114.5	146.6
19		112.6	95.0	120.7
20		115.4	100.5	124.9
21		92.6	78.8	97.6
22		86.2	78.2	95.9
23		83.2	63.8	79.0
24		93.8	46.0	60.0
25		110.0	69.6	78.3

Table 3. Cont.



No.	X	T _{MP}	T _{N_{TB}-N}	T _{N-Iso}
26		95.6	100.0	123.8
27		102.2	61.2	72.8
28		88.7	80.7	95.1
29		91.9	85.2	110.0

Turning now to variations in the linking groups and spacer regions, while the N_{TB} phase is most commonly associated with dimers incorporating a methylene spacer, it is also found in a large number of materials with imine linking units. The imine-linked (3-hydroxyphenyl) 4-alkylbenzoate dimers reported by Šepelj et al. (Table 4) showed a delicate balance between columnar, nematic, and N_{TB} mesophases, with the specific phase type being dependent upon both the length of the central spacer as well as the peripheral alkyl chains [50].

Table 4. Transition temperatures (T_{A-B}, °C) of some imine-linked phenyl 4-alkoxybenzoate dimers [51–53].


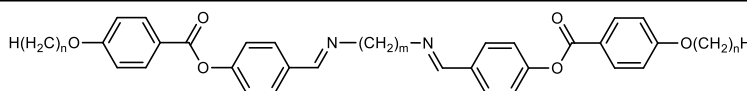
No.	n	m	T _{MP}	T _{Col-N/Iso}	T _{N_{TB}-N}	T _{N-Iso}
30	4	5	106	-	-	102
31	6	5	113	-	87	97
32	8	5	103	99	-	102
33	10	5	105	111	-	-
34	12	5	107	116	-	-
35	14	5	105	120	-	-
36	4	7	119	-	-	121
37	6	7	98	-	93	113
38	8	7	103	-	-	110
39	10	7	97	106	-	108
40	12	7	100	112	-	-
41	14	7	99	117	-	-

Analogous in structure to the materials shown in Table 5, Šepelj et al. reported a family of imine linked phenyl 4-alkoxybenzoate dimers. Only one member displayed the twist-bend nematic phase, with $m = 7$ and $n = 4$, the majority of the materials displaying a B6 type mesophase.

We now explore the role of the chemical makeup of the central spacer beyond the methylene and imine systems already discussed. Archbold et al. reported a family of cyanobiphenyl dimers that are homologous to CB7CB in structure, having spacers of comparable length (seven methylene or equivalent units) but with different chemical makeup (Table 6) [54]. Materials incorporating two alkyne units were non-mesogenic. The onset temperature of the N_{TB} phase was significantly reduced for the dipropyl ether spacer (55), while the N_{TB} phase was absent for 61, which included a diethyleglycol spacer. The *bis* imine material 60 exhibited a direct N_{TB} to isotropic transition temperature. Archbold et al. linked the observed transition temperatures to the average bend of the molecule, itself obtained as a probability weighted average of many conformers obtained with the

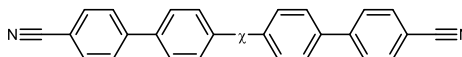
rotational isomeric state (RIS) approximation, with the suggestion that an ‘optimal’ bend angle exists for the N_{TB} phase, which leads to, *inter alia*, direct N_{TB} –Iso transitions. This is exemplified by the high thermal stabilities of the N_{TB} phases of the ketone-linked material (CBK-5-KCB) as well as the imine-linked material (CBI-3-ICB).

Table 5. Transition temperatures (T_{A-B} , °C) of salicyaldimine dimers with odd spacer parity [50].



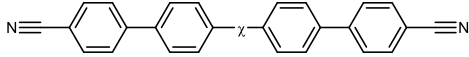
No.	<i>n</i>	<i>m</i>	T_{MP}	$T_{B6-N/Iso}$	$T_{N_{TB}-N}$	T_{N-Iso}
42	4	5	114.0	99.1	-	102.0
43	6	5	123.5	116.9	-	-
44	8	5	94.2	121.0	-	-
45	10	5	88.5	109.5	-	-
46	12	5	96.2	96.1	-	-
47	14	5	101.2	-	-	-
48	4	7	112.2	84.4	96.6	115.0
49	6	7	96.4	114.7	-	-
50	8	7	111.2	119.5	-	-
51	10	7	100.1	110.1	-	-
52	12	7	90.9	99.3	-	-

Table 6. Transition temperatures (T_{A-B} , °C) of cyanobiphenyl derivatives with varying central spacer composition, equivalent to heptamethylene [54].



No.	Name	χ	T_{MP}	$T_{N_{TB}-N}$	T_{N-Iso}	Ave. Bend/ $^{\circ}$
53	CBT3TCB	---≡---(CH ₂) ₃ ---≡---	160.5	-	-	n/r
54	CBT1O1TCB	---≡---O---≡---	>225	-	-	n/r
4	CB7CB	---(CH ₂) ₇ ---	104.4	105.5	118.9	103.5
55	CB3O3CB	---(CH ₂) ₃ O(CH ₂) ₃ ---	100.5	46.0	68.0	91.0
56	CBT4OCB	---≡---(CH ₂) ₄ O---	132.8	97.0	145.2	100.5
57	CB6OCB	---(CH ₂) ₆ O---	102.1	110.5	154.2	104.4
58	CBO5OCB	---O(CH ₂) ₅ O---	137.9	81.3	189.2	102.9
59	CBK5KCB	---C(=O)---(CH ₂) ₅ ---C(=O)---	158.1	145.1	189.4	108.2
60	CBI3ICB	---N---(CH ₂) ₃ ---N---	170.8	114.9	-	115.1
61	CBO2O2OCB	---O(CH ₂) ₂ O(CH ₂) ₂ O---	150.5	-	157.8	104.5

Refining the earlier approach of Archbold et al., Mandle and Goodby investigated the conformational preference of a series of homologues of CB9CB (Table 7) [55,56]. Again, the rotational isomeric state approximation was used to generate conformational libraries for each material; the average bend angle between the two mesogenic units then being calculated as a probability weighted average. Conformational ensembles were validated by comparison of average inter-proton distances with those obtained from ^1H - ^1H NOESY NMR experiments. It is suggested that the stability of the N_{TB} phase is related to the average bend angle, specifically, a high ratio of $T_{N_{TB}-N}$ to T_{N-Iso} is achieved by having an average bend angle in excess of 110° .

Table 7. Transition temperatures (T_{A-B} , °C) of cyanobiphenyl derivatives with varying central spacer composition, equivalent to nonamethylene [54–58]. * Glass to N_{TB} transition.


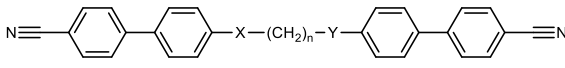
No.	Name	χ	T_{MP}	$T_{N_{TB}-N}$	T_{N-Iso}	Ave. Bend/ $^{\circ}$
6	CB9CB	---(CH ₂) ₉ ---	83.3	105.4	121.5	103.1
62	CBI7ICB	---N(CH ₂) ₇ N---	140.8	114.7	138.7	111.5
63	CB8KCB	---(CH ₂) ₈ ---	127.8	128.1	153.9	98.5
64	CBT6OCB	---≡(CH ₂) ₆ O---	137.1	102.0	153.6	98.5
65	CB8OCB	---(CH ₂) ₈ O---	110.6	109.9	153.3	100.7
66	CBS7SCB	---S(CH ₂) ₇ S---	15.9 *	88.3	115.2	99.2
67	CBS7OCB	---S(CH ₂) ₇ O---	55.0	95.9	146.7	96.8
68	CBS ₇ SeCB	---Se(CH ₂) ₇ Se---	80.8	43.1	71.9	98.8
69	CBcZ5OCB	---O(CH ₂) ₅ O---	95.1	39.8	91.3	93.0
70	CBcO5OCB	---O(CH ₂) ₅ O---	122.4	71.3	129.9	96.8
71	CBO7OCB	---O(CH ₂) ₇ O---	120.0	-	-	-
72	CBT5CBT	---≡(CH ₂) ₅ ≡---	169.1	-	-	-

We now consider four families of related cyanobiphenyl dimers with varying linking groups and spacer lengths (Table 8) [59–61]. The chemical makeup of each family is evident from their names (e.g., the $CBnOCB$ series feature one methylene and one ether linking unit, the $CBnSCB$ series feature one methylene and one thioether linking unit, and so on). Further examples from each family are to be found in the given references. Generally, the transition temperatures of thioether containing materials are lower than the equivalent $CBnOCB$ material, with the difference being most pronounced for shorter spacer lengths. A simple explanation suffices here, with a deeper understanding needing to draw on other relevant conformational effects. Consider that a methylene unit imparts a tetrahedral bond angle (109.5°), an ether gives an angle of 104.5° , but an arylthioether has a bond angle of $\sim 90^{\circ}$. The influence of thioethers is therefore most pronounced for shorter chain lengths, whereas for longer spacers, they are somewhat offset. The thioether is somewhat unfavourable for the formation of the N_{TB} phase as it tends to depress the average bend angle away from the apparent favoured value of $>110^{\circ}$. However, for some materials (CBO7SCB, 67, and CBS7SCB, 66) the melting point is suppressed to such a degree that the materials are in the N_{TB} phase at ambient temperature, which is a remarkable achievement that greatly simplifies experimentation. The helical pitch length of several compounds in Table 8 has been reported: CB6OCB ~ 10 – 15 nm [62], CBS7SCB 8.7 nm, CBO7SCB 18.4 nm, and CBO5SCB 14.8 nm [63]. Linking the N_{TB} pitch length to molecular geometric parameters appears to be a logical future direction. Almost simultaneously with Arakawa et al. [61], the $CBSnSCB$ and CBO_nSCB materials were also synthesised and reported independently by Imrie et al. [64]. Imrie et al. also reported the pitch lengths of CBO5SCB (~ 8.9 nm), CBS7SB (~ 8.7 nm), and the mixed cyanoterphenyl/cyanobiphenyl material, CT6SCB (~ 9.7 nm); in all three cases, this corresponded to approximately four end-to-end molecular lengths.

Arakawa et al. subsequently demonstrated cyanobiphenyl dimers with mixed thioether/ketone linking units [65] (Table 9). Earlier, Archbold et al. found that ketone-linking units generated highly stable N_{TB} phases due to their favourable bend angles (Table 6) [54]. Employing mixed ketone and thioether units showed a dramatic increase in the N_{TB} onset temperature when compared to the equivalent materials employing either two thioethers ($CBSnSCB$), or one thioether and one other linking unit ($CBnSCB$, CBO_nSCB , $CBSnSCB$). Again, a simple explanation suffices for the sake of this review: the ketone unit has a bond angle of $\sim 120^{\circ}$, which offsets the unfavourable angle imposed by the thioether. Clearly, a detailed DFT study of the conformational landscape of these materials (and in-

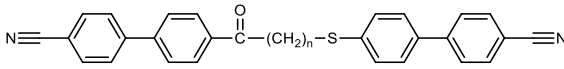
deed, others) appears warranted, and presents one possible route to further understanding these intriguing materials.

Table 8. Transition temperatures (T_{A-B} , °C) of cyanobiphenyl derivatives with methylene, ether, or thioether linking groups and varying spacer length: selected members of the $CBnOCB$ [59,60], $CBnSCB$ [61], CBO_nSCB [61], and CBS_nSCB [61] series. * Glass to N_{TB} transition.



No.	Name	n	X	Y	T_{MP}	$T_{N_{TB-N}}$	T_{N-Iso}
73	CB4OCB	3	-CH ₂ -	-O-	121	103	143
74	CB4SCB	3	-CH ₂ -	-S-	126.2	70.3	86.8
75	CBO3SCB	3	-O-	-S-	101.1	47	137.5
76	CBS3SCB	3	-S-	-S-	70.1	44.0	83.2
77	CB6OCB	5	-CH ₂ -	-O-	99	109	155
78	CB6SCB	5	-CH ₂ -	-S-	99.0	89.6	113.2
79	CBO5SCB	5	-O-	-S-	59.5	90.1	143.8
80	CBS5SCB	5	-S-	-S-	68.9	78.0	107.8
65	CB8OCB	7	-CH ₂ -	-O-	112	108	154
81	CB8SCB	7	-CH ₂ -	-S-	92.6	93.9	117.8
67	CBO7SCB	7	-O-	-S-	16.0 *	95.9	146.7
66	CBS7SCB	7	-S-	-S-	15.9 *	88.3	115.2
82	CB9OCB	9	-CH ₂ -	-O-	116	107	148
83	CB9SCB	9	-CH ₂ -	-S-	103.4	95.5	119.0
84	CBO9SCB	9	-O-	-S-	98.0	95	143.0
85	CBS9SCB	9	-S-	-S-	100.8	89	116.7

Table 9. Transition temperatures (T_{A-B} , °C) of cyanobiphenyl derivatives with mixed ketone/thioether linking units [65].



No.	Name	n	T_{MP}	$T_{N_{TB-N}}$	T_{N-Iso}
86	CBK3SCB	3	114.6	104.6	132.6
87	CBK5SCB	5	120.9	110.0	152.3
88	CBK7SCB	7	121.8	113.6	152.1
89	CBK9SCB	9	155.8	-	145.0

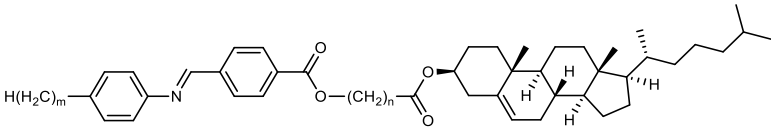
3. Chiral N_{TB} Materials

The N_{TB} phase has been described as the “structural link” between the conventional nematic phase and the helical chiral nematic (cholesteric) phase [10]. As discussed, the N_{TB} phase has a helical structure and when formed from achiral molecules, there is no preference for left- or right-handed helices. Our focus in this review was on molecular structure and the materials that generate the N_{TB} phase, so our focus was on examples whereby chirality results from the molecular structure of the dimer itself, rather than systems in which chirality is introduced via an additive [66].

Gorecka et al. reported a number of ester-linked unsymmetrical dimers that incorporated cholesterol as a mesogenic unit; these materials are chiral, and thus they are the first reported chiral N_{TB} materials. The length of the central spacer and its parity dictate the balance between exhibiting N_{TB} (odd parity) or SmA (even parity) mesophases in these materials. The mesophase behaviour of these materials is more complex than shown in Table 10, with the materials exhibiting multiple nematic phases and/or blue phases. The N_{TB} pitch length of **90** was measured to be 50 nm by in situ AFM, notably larger than that of CB7CB, but still about a few molecular lengths [24,67]. Later, the helical pitch length of

99 was measured by resonant carbon K-edge X-ray scattering and found to take a value of ~ 11 nm [68]. The pitch length of the chiral nematic phase was determined to be 224 nm by the same method.

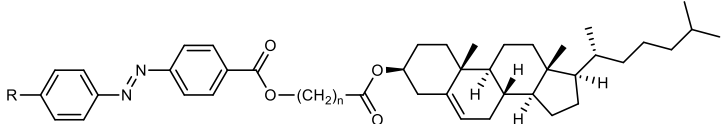
Table 10. Transition temperatures (T_{A-B} , °C) of unsymmetrical cholesterol containing dimers.



No.	n	m	T_{MP}	T_{SmA-N^*}	$T_{N_{TB}-N^*}$	T_{N^*-Iso}
90	3	1	112.3	-	55.1	67.7
91	4	1	127.9	146.9	-	191.8
92	5	1	92.5	-	67.9	102.3
93	6	1	152.3	120.0	-	158.4
94	7	1	83.0	-	75.7	110.8
95	9	1	81.2	-	75.7	113.6
96	10	1	82.7	-	-	137.5
97	15	1	62.9	-	63.2	107.9
98	5	2	74.0	-	60.6	93.6
99	5	3	77.5	-	62.2	98.8
100	5	4	44.2	71.9	-	99.3

Gorecka et al. also reported another family of cholesterol containing dimers that exhibited the N_{TB} phase (Table 11), with some members also exhibiting a smectic phase of unknown structure (SmX) [24]. The pitch length of **104** in the N_{TB} phase was measured by the resonant X-ray scattering method, with a temperature dependent value of 13.3–20.3 nm. Conversely, the chiral nematic pitch length for this material was measured by the same technique to be 220 nm [68]. Although not reported upon, the incorporation of an azo unit presumably enables isothermal N_{TB} transitions in these materials (*via* photoisomerisation), as first reported by Paterson et al. [69].

Table 11. Transition temperatures (T_{A-B} , °C) of unsymmetrical dimers comprising cholesterol and azobenzene units.

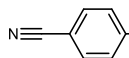
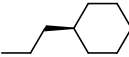
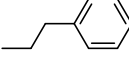
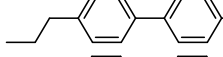
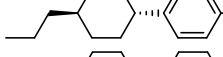
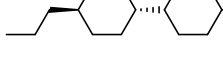
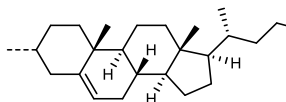


No.	n	R	T_{MP}	T_{SmX-N^*}	$T_{N_{TB}-N^*}$	T_{N^*-Iso}
101	5	-CH ₃	83.4	-	67.1	105.5
102	5	-OCH ₃	84.3	-	80.8)	124.9
103	5	-OC ₂ H ₅	107.0	97.6	-	134.4
104	7	-CH ₃	63.9	-	74.0	111.5
105	9	-CH ₃	69.6	-	75.8	113.6
106	15	-CH ₃	60.5	60.3	-	100.3

Mandle and Goodby reported the synthesis of symmetrical LC dimers in which the central spacer is itself chiral (Table 12); starting from (*R*)-2-methylglutaric acid, four synthetic steps telescoped into two reactions afforded the key (*R*)-bis-1,5-(4-hydroxyphenyl)-2-methylpentane intermediate, which was elaborated using standard esterification protocols, affording compounds **107**–**113**. The measured helical twisting power of **107** was rather low ($0.36 \text{ mm}^{-1} \text{ wt}\%^{-1}$) due to the large degree of conformational freedom experienced by the lateral methyl unit. The N_{TB} phase was only exhibited by materials whose mesogenic units had a large aspect ratio due to the unfavourable conformational effects of the lateral

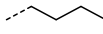
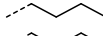
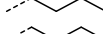
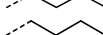

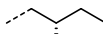
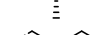

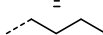
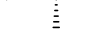
methyl unit within the central spacer. However, this also gave rise to the unusual SmA–N_{TB} transition in compounds **111** and **112**, which has previously only been observed for a small handful of materials [70].

Table 12. Transition temperatures (T_{A-B} , °C) of symmetrical dimers containing an (R)-2-methylpentamethylene spacer.

No.	R	T _{MP}	T _{SmA-N_{TB}*}	T _{N_{TB}-N*}	T _{N*-Iso}
107		134.1	-	-	71.1
108		61.6	-	-	-
109		69.1	-	-	-
110		66.6	-	-	233.6
111		117.1	110.8	123.5	219.8
112		119.3	161.0	167.2	236.4
113		123.3	-	-	237.4

Walker et al. reported a family of unsymmetrical dimers that are terminated by either butyl, racemic 2-methylbutyl, or (S)-2-methylbutyl chains (Table 13) [71]. The N_{TB}–N transition temperature was marginally higher for chiral materials than the achiral analogues, in agreement with the theoretical predictions [72]. Notably, the N_{TB} phase formed by **119** was found to be miscible with that of the achiral material CB6OCB (77).

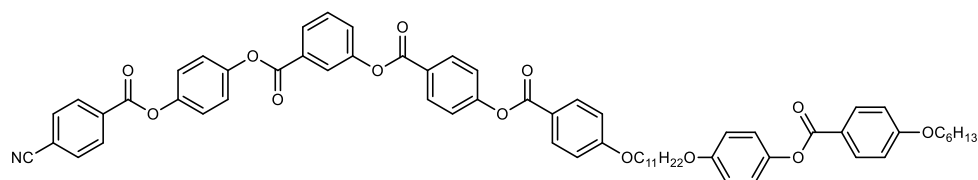
Table 13. Transition temperatures (T_{A-B} , °C) of unsymmetrical CBnOPZPZP dimers with a terminal butyl, (S)-2-methylbutyl, or *rac* 2-methylbutyl chain [71].

No	<i>n</i>	<i>m</i>	T _{MP} /°C	T _{SmA-N_{TB}*}	T _{N_{TB}-N*}	T _{N*-Iso}
114	4		154	-	-	249
115	6		154	-	96	248
116	8		144	-	93	241
117	10		135	-	89	231
118	4		162	-	-	209
119	6		153	-	89	214
120	8		132	-	93	212
121	10		131	88	-	203
122	6		153	-	85	214
123	8		131	-	92	207

4. Bent-Core Systems

Compared to dimers comprising rod-like (calamitic) mesogenic units, there are relatively few examples of bent-core liquid crystals that exhibit the N_{TB} phase. A family of non-symmetrical bent-core materials with a central phenyl piperazine group were prepared by Schroder et al. [73] with shorter homologues exhibiting two nematic phases, denoted as N_X . Longer chain homologues exhibited the SmC_P phase. Later, compound **126** was studied by FFTEM, and the lower temperature nematic was shown to be a N_{TB} phase with a pitch length of 14 nm—larger than CB7CB, but of the order of a few molecular lengths [12]. Based on this, it seems probable that the ' N_X ' phase of compounds **124** and **125** is also the N_{TB} phase.

Tamba et al. reported an ether-linked dimer, comprising a bent-core unit as well as a calamitic unit, which exhibited the twist-bend nematic phase as well as an unidentified ' M_2 ' mesophase [74]. Homologues employing other spacer lengths (trimethyleneoxy or hexamethyleneoxy) or a dodecyloxy terminal chain *in lieu* of the nitrile unit employed in **134** do not exhibit the twist-bend nematic phase. To date, compound **134** (Figure 2), along with those in Table 14, are the only known examples of bent-core materials that exhibit the twist-bend nematic phase, although others have been previously suggested [75].



134: Cr 136 (M_2 109 N_{TB} 115) N 145 Iso

Figure 2. Chemical structure and transition temperatures ($^{\circ}C$) of the hybrid bent-core/calamitic dimer reported by Tamba et al. [74]. Phase transitions are presented in parenthesis are monotropic.

Table 14. Transition temperatures (T_{A-B} , $^{\circ}C$) of N-phenyl piperazine derived bent-core compounds [12,73].

No.	n	T_{MP}	$T_{SmC_P-N/Iso}$	T_{Col_X-N}	$T_{N_{TB}-N}$	T_{N-Iso}
124	4	201	-	-	193	212
125	5	187	-	-	172	192
126	6	176	-	157	169	188
127	7	169	-	-	-	186
128	8	177	180	-	-	180.5
129	9	167	185	-	-	-
130	10	162	191	-	-	-
131	11	161	194	-	-	-
132	12	165	201	-	-	-
133	16	142	193	-	-	-

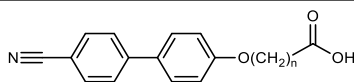
5. Beyond Dimers: Trimers, Tetramers and Oligomers

Now, our focus shifts beyond covalent dimers to equivalent trimers, tetramers, and so on [76–85]. We will focus first on materials of special note before considering the behaviour of families of materials. CB6OBA, a hydrogen bonded LC-trimer, was the first oligomeric material shown to exhibit the N_{TB} phase (Table 15) [86]. The hexamethyleneoxy spacer

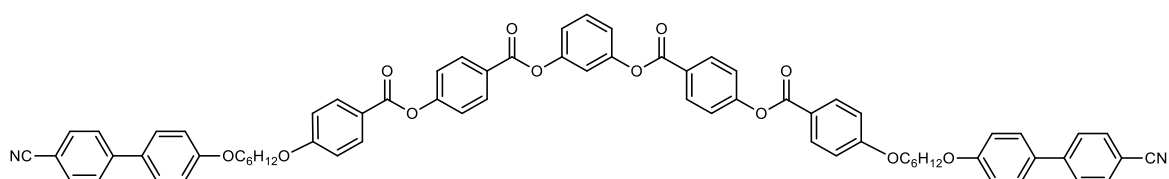
of CB6OBA imparts a gross bent shape to the hydrogen bonded dimer, permitting the formation of the N_{TB} phase, which is absent for the even parity homologue, CB5OBA. The terminal carboxylic acid group contains a hydrogen bond donor and acceptor, thus, both open and closed forms can be observed [87,88].

Table 15. Transition temperatures (T_{A-B} , °C) of the hydrogen-bonded trimers CB5OCB (linear) and CB6OBA (bent) [86].

No.	Name	n	T_{MP}	$T_{N_{TB-N}}$	T_{N-Iso}
135	CB5OBA	5	196	-	209
136	CB6OCB	6	160	159	197



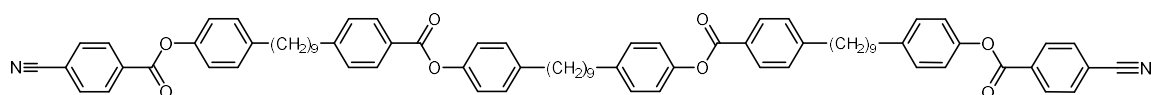
Wang et al. reported a symmetrical trimer that features two cyanobiphenyl units appended to a bent-core [13]; curiously, spacers in this system have even parity, with the requisite bent shape resulting from the 1,3-disubstituted phenyl ring employed within the bent-core unit. The pitch length of the N_{TB} phase of **137** (Figure 3) was measured to be 19 nm using the FFTEM method, which was roughly four molecular lengths. X-ray scattering showed that the nematic phase is intercalated, with the d-spacing of the diffuse small angle peak being at $\sim 1/3$ of the molecular length. The orientational order parameters $\langle P_2 \rangle$ and $\langle P_4 \rangle$ were measured by X-ray scattering, both being found to decrease on entering the N_{TB} phase. Replacement of a single cyanobiphenyl with a decyloxy chain was shown to eliminate the N_{TB} phase [89].



137: Cr n/r N_{TB} 80 N 235 Iso

Figure 3. Chemical structure and transition temperatures (°C) of the hybrid bent-core/calamitic trimer (**137**) reported by Wang et al. [13]. The melting point was not reported.

In 2016, Mandle and Goodby reported a methylene linked tetramer comprising phenyl benzoate mesogenic units (Figure 4) [47,90]. The heliconical tilt angle of the N_{TB} phase of **138** was estimated via the X-ray scattering method, and was found to be comparable to the parent dimer, compound **11** (Table 2) [42]. The synthetic strategy used to prepare this tetramer was further refined to deliver a twist-bend nematic hexamer, with six mesogenic units connected in a linear manner.

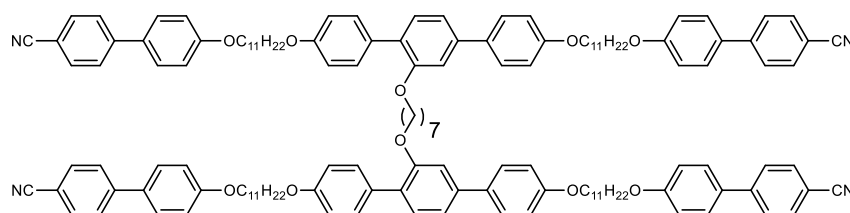


138: Cr 113.6 N_{TB} 127.7 N 141.5 Iso

Figure 4. Chemical structure and transition temperatures (°C) of the linear tetramer reported by Mandle and Goodby.

So far, all of the materials encountered have had a linear sequence of mesogenic units. The hexamer **139** features two trimers appended via a central heptamethylenedioxy spacer (Figure 5) [91]. The individual trimers are themselves mesogenic and display the N_{TB}

phase; however, the N_{TB} -N transition occurs at a significantly higher temperature in the duplexed hexamer [91].



139: Cr 123.7 N_{TB} 117.2 N 172.9 Iso

Figure 5. Chemical structure and transition temperatures ($^{\circ}\text{C}$) of the non-linear hexamer reported by Mandle and Goodby.

Jákli et al. reported a homologous family of 2',3'-difluoroterphenyls [92], from the simple monomer ($n = 0$, **140**, Table 16) to the homologous tetramer **143**. Some homologous dimers, with varying terminal/spacer chain length, have also been reported [93–95], and a wealth of investigations have been performed on this family of materials [96–98].

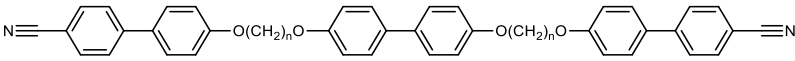
Table 16. Transition temperatures (T_{A-B} , $^{\circ}\text{C}$) of compounds **140–143**, the 'DTC5-C9' family [92].

No.	n	T_{MP}	T_{SmX-N}	$T_{N_{TB}-N}$	T_{N-Iso}
140	0	34	-	-	116.5
141	1	77	85	124	162
142	2	127	-	145	192
143	3	142	-	168	205

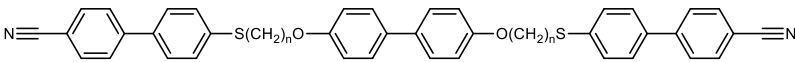
The monomeric material displays only a nematic phase whereas those with two or more mesogenic units display nematic and N_{TB} phases, with the transition temperature increasing as the number of mesogenic units is increased. So far, we have considered odd–even effects as being restricted to those resulting from the parity of the central spacer. However, for the 'DTC5-C9' family, Jákli et al. showed remarkable odd–even effects in birefringence, bend elastic constants, and X-ray scattering, which resulted from the number of mesogenic units [92].

Arakawa et al. reported two families of symmetrical liquid crystalline trimers featuring ether (CBO n OBO n OCB, Table 17) [99] and mixed ether/thioether (CBS n OBO n SCB, Table 18) [100] linking groups, but with varying spacer lengths. For a given chain length, the former family exhibited higher transition temperatures than the latter. In both families, materials of even parity displayed nematic and smectic A phases, whereas those of odd parity showed nematic and N_{TB} phases.

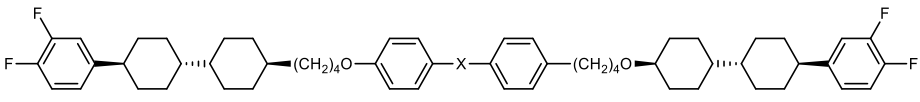
Al-Janabi and Mandle reported a set of liquid crystalline trimers that incorporated various saturated hydrocarbon rings, isosteric with 1,4-disubstituted benzene (Table 19) [101]. Only the 2,6-cuneane material did not exhibit the N_{TB} phase, and this was attributed to the unfavourable bend angles imposed by this non-linear motif. For the materials that exhibited the N_{TB} phase ($X = 1,4$ -benzene, 1,4-cyclohexane, and 1,4-cubane), the heliconical tilt angle was found to be effectively independent of the chemical makeup of the central ring.

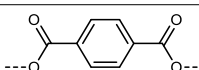
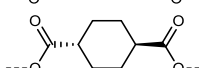
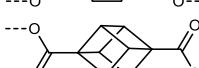

Table 17. Transition temperatures (T_{A-B} , °C) of ether-linked trimers **144–151** [99].


No.	n	T_{MP}	T_{SmA-N}	$T_{N_{TB}-N}$	T_{N-Iso}
144	4	230.1	197	-	297.4
145	5	176.6	-	122	215.4
146	6	217.4	192	-	257.8
147	7	162.9	-	132	207.2
148	8	201.0	175	-	231.9
149	9	155.0	-	135	195.8
150	10	198.0	150	-	210.8
151	11	147.4	-	130.5	185.9

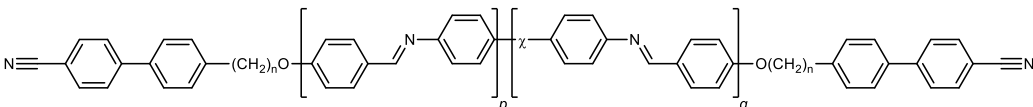
Table 18. Transition temperatures (T_{A-B} , °C) of mixed ether/thioether linked trimers **152–160** [100].


No.	n	T_{MP}	T_{SmA-N}	$T_{N_{TB}-N}$	T_{N-Iso}
152	3	186.4	-	-	142.0
153	4	235.3	-	-	253.2
154	5	171.8	-	117	154.2
155	6	219.0	180	-	217.4
156	7	149.4	-	126	162.4
157	8	195.6	167	-	198.8
158	9	131.3	-	122.7	158.8
159	10	184.8	146	-	176.2
160	11	135.4	-	121	154.4

Table 19. Transition temperatures (T_{A-B} , °C) of compounds **161–164**; # sample decomposes at and above 230 °C [101].


No.	X	T_{MP}	$T_{N_{TB}-N}$	T_{N-Iso}
161		178.8	166.2	304.6
162		169.3	159.8	285.5
163		174.4	163.9	>230 #
164		162.2	-	>230 #

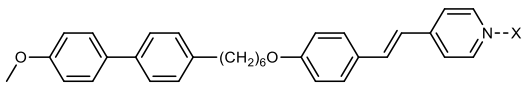
The relationship between the stability of the N_{TB} phase and oligomer shape was studied in detail for a family of cyanobiphenyl/benzylideneaniline oligomers (Table 20) [102]. Due to the explored variations in the composition and parity of the spacer units, neighbouring mesogenic units within this family can have both ‘bent’ or ‘linear’ configurations. While all materials exhibit the N_{TB} phase, the helical pitch length has a strong dependence on the gross molecular shape; the all bent material **166** has three odd-parity spacers and a pitch of 7 nm, the bent-linear-bent tetramer **170** has a pitch of 12 nm, and the linear-bent-linear tetramer **172** has a pitch length of ~17 nm.

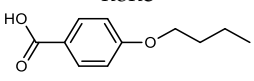
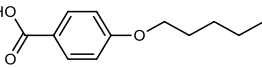
Table 20. Transition temperatures (T_{A-B} , °C) of compounds **77**, **165–172**. *Link Seq.* refers to the shape (B = bent, L = linear) shape of the all *trans* conformation of the linkage units [102].


No.	<i>n</i>	<i>X</i>	<i>p</i>	<i>q</i>	T_{MP}	$T_{N_{TB-N}}$	T_{N-Iso}	Link Seq.
77	6	-	0	0	99	109	155	<i>B</i>
165	6	-	1	0	153	142	185	<i>BB</i>
166	6	-(CH ₂) ₇ -	1	1	140	159	180	<i>BBB</i>
167	6	-(CH ₂) ₆ O-	1	1	151	158	195	<i>BBB</i>
168	6	-	1	1	156	162	215	<i>BBB</i>
169	6	O(CH ₂) ₆ O-	1	1	166	166	235	<i>BLB</i>
170	6	-(CH ₂) ₈ -	1	1	131	152	212	<i>BLB</i>
171	7	-(CH ₂) ₇ -	1	1	145	132	225	<i>LBL</i>
172	O6	-(CH ₂) ₇ -	1	1	131	143	242	<i>LBL</i>

6. Supramolecular N_{TB} Materials

We now consider supramolecular LC dimers that result from non-covalent bonds, both achiral and chiral, which exhibit the N_{TB} phase. The hydrogen bonded-LC trimer *CB6OBA* was the first reported supramolecular N_{TB} material, however, as the complex incorporates two identical molecules, there is no scope for tunability of structure. Walker et al. demonstrated a remarkable pair of supramolecular LC dimers that incorporates dissimilar hydrogen bond acceptors and donors. The parent 4-methoxybiphenyl/stilbazole dimer (**173**) is non-mesogenic; complexation with either 4-butoxy- or 4-pentyloxybenzoic acid affords the isolable supramolecular complexes shown in Table 21, both of which exhibit the N_{TB} phase [103]. While many materials are known to exhibit transitions from the N_{TB} phase to tilted (*SmC*, *vide infra*) or heliconical (*SmC_{TB}*) [104] phases, complex **175** is unusual in that it exhibits a transition from the N_{TB} phase to an orthogonal smectic A phase, as do compounds **111** and **112**.

Table 21. Transition temperatures (T_{A-B} , °C) of compound **173** and complexes **174** and **175** [103].


No.	<i>X</i>	T_{MP}	T_{SmX}	$T_{SmA-N_{TB}}$	$T_{N_{TB-N}}$	T_{N-Iso}
173	none	142.8	-	-	-	-
174		121.9	86.2	-	109.4	166.4
175		112.0	85.5	93.5	98.0	157.7

This design strategy was also used to deliver chiral supramolecular N_{TB} materials by use of the cyanobiphenyl/stilbazole system with an appropriate chiral benzoic acid [105]. The transition temperatures for this chiral supramolecular complex are somewhat lower than those of the linear analogue (shown in Table 22), and this depression of transition temperatures by branched alkyl chains is a general phenomenon in LC dimers. Resonant soft X-ray scattering at the carbon K-edge was used to measure the pitch length of **176**,

which was found to take a temperature dependent value of 8.1–8.4 nm, or around two complex lengths.

Table 22. Transition temperatures (T_{A-B} , °C) of complexes **176** and **177** [105].

No.	X	$T_{MP}/^{\circ}C$	$T_{N_{TB}-N}/^{\circ}C$	$T_{N-Iso}/^{\circ}C$
176		107	95	167
177		103	88	145

Walker et al. subsequently demonstrated the CB6OCB:*n*OS series of materials, utilising the benzoic acid/stilbazole system [106]. A weak odd–even effect was seen for both the $N_{TB}-N$ and $N-Iso$ transition temperatures. Homologues with longer terminal chain length ($n \geq 4$) also exhibited smectic C phases. For homologues with longer chains still ($n \geq 8$, not shown in Table 23), the N_{TB} phase was absent, instead, the materials showed SmA and SmA_B phases [106].

Table 23. Transition temperatures (T_{A-B} , °C) of complexes **178–184** [106].

No.	<i>n</i>	T_{MP}	$T_{SmC-N_{TB}}$	$T_{N_{TB}-N}$	T_{N-Iso}
178	1	130	-	110	182
179	2	119	-	115	190
180	3	109	-	108	173
181	4	108	86	113	180
182	5	121	92	107	165
183	6	105	96	106	158
184	7	100	100	104	155

In the same paper, further elaboration of the cyanobiphenyl/stilbazole system to unsymmetrical supramolecular trimers comprising CB6OBA and a stilbazole dimer was reported (Table 24). Although the two materials differed in their melting point, the $N_{TB}-N$ and $N-Iso$ transitions were only slightly different. We note that, although examples are presently limited to hydrogen bonded systems, there is no obvious reason why other types of non-covalent interactions could not be employed in the design of N_{TB} materials (e.g., halogen bonds [107]), and presents a logical avenue for future research.

Table 24. Transition temperatures (T_{A-B} , °C) of complexes **185** and **186** [106].

No.	X	T_{MP}	$T_{N_{TB}-N}$	T_{N-Iso}
185	-CN	127	143	186
186	-OCH ₃	140	142	184

7. Summary and Outlook

The decade since the experimental discovery of the N_{TB} phase by Cestari et al. has seen a resurgence of interest in liquid crystalline dimers and oligomers. Recently, there has been a notable move from symmetrical methylene-linked dimers to more complex forms: chiral systems, photoresponsive dimers, supermolecular materials, higher and non-linear oligomers, and polymers. The recent development of room temperature materials greatly facilitates the exploration of the rich physics of these systems.

General design principles for N_{TB} materials are always evolving; with the ability to tune molecular bend/shape through synthetic chemistry, the ability to prepare oligomers, and supramolecular systems, it is possible to obtain twist-bend nematic materials through rational design rather than through ad hoc experimentation. This being said, the majority of twist-bend nematic materials follow the tried-and-tested formula of end-to-end appended mesogenic units, with only a handful of bent-core materials and a single non-linear oligomer falling outside of this description. It is interesting to speculate as to whether more unconventional molecular geometries (e.g., lambda shaped trimers, mixed rod-disk architectures) are capable of supporting twist-bend nematic order.

Different materials display rather different helix pitches that themselves evolve differently over temperature; an understanding of this from a molecular perspective is currently elusive, but appears a reasonable proposition for future work. The potential for incorporating stimuli responsive groups, coupled with the remarkable physical properties of this phase of matter, suggests that interest in this area will continue for some time.

Funding: R.J.M. acknowledges funding from UK Research and Innovation (UKRI).

Conflicts of Interest: The author declares no conflict of interest.

References

1. Freiser, M.J. Ordered states of a nematic liquid. *Phys. Rev. Lett.* **1970**, *24*, 1041–1043. [[CrossRef](#)]
2. Yu, L.J.; Saupé, A. Observation of a biaxial nematic phase in potassium laurate-1-decanol-water mixtures. *Phys. Rev. Lett.* **1980**, *45*, 1000–1003. [[CrossRef](#)]
3. Mandle, R.J.; Cowling, S.J.; Goodby, J.W. A nematic to nematic transformation exhibited by a rod-like liquid crystal. *Phys. Chem. Chem. Phys.* **2017**, *19*, 11429–11435. [[CrossRef](#)]
4. Nishikawa, H.; Shiroshita, K.; Higuchi, H.; Okumura, Y.; Haseba, Y.; Yamamoto, S.I.; Sago, K.; Kikuchi, H. A fluid liquid-crystal material with highly polar order. *Adv. Mater.* **2017**, *29*, 1702354. [[CrossRef](#)]
5. Mertelj, A.; Cmok, L.; Sebastián, N.; Mandle, R.J.; Parker, R.R.; Whitwood, A.C.; Goodby, J.W.; Čopič, M.J.P.R.X. Splay nematic phase. *Phys. Rev. X* **2018**, *8*, 041025. [[CrossRef](#)]
6. Sebastian, N.; Cmok, L.; Mandle, R.J.; de la Fuente, M.R.; Drevensek Olenik, I.; Copic, M.; Mertelj, A. Ferroelectric-ferroelastic phase transition in a nematic liquid crystal. *Phys. Rev. Lett.* **2020**, *124*, 037801. [[CrossRef](#)]
7. Chen, X.; Korblova, E.; Dong, D.; Wei, X.; Shao, R.; Radzihovsky, L.; Glaser, M.A.; Maclennan, J.E.; Bedrov, D.; Walba, D.M.; et al. First-principles experimental demonstration of ferroelectricity in a thermotropic nematic liquid crystal: Polar domains and striking electro-optics. *Proc. Natl. Acad. Sci. USA* **2020**, *117*, 14021–14031. [[CrossRef](#)]
8. Dozov, I. On the spontaneous symmetry breaking in the mesophases of achiral banana-shaped molecules. *Europhys. Lett.* **2001**, *56*, 247–253. [[CrossRef](#)]
9. Cestari, M.; Diez-Berart, S.; Dunmur, D.A.; Ferrarini, A.; de la Fuente, M.R.; Jackson, D.J.; Lopez, D.O.; Luckhurst, G.R.; Perez-Jubindo, M.A.; Richardson, R.M.; et al. Phase behavior and properties of the liquid-crystal dimer 1'',7''-bis(4-cyanobiphenyl-4'-yl) heptane: A twist-bend nematic liquid crystal. *Phys. Rev. E Stat. Nonlinear Biol. Soft Matter Phys.* **2011**, *84*, 031704. [[CrossRef](#)]
10. Borshch, V.; Kim, Y.K.; Xiang, J.; Gao, M.; Jakli, A.; Panov, V.P.; Vij, J.K.; Imrie, C.T.; Tamba, M.G.; Mehl, G.H.; et al. Nematic twist-bend phase with nanoscale modulation of molecular orientation. *Nat. Commun.* **2013**, *4*, 2635. [[CrossRef](#)]
11. Chen, D.; Porada, J.H.; Hooper, J.B.; Klitnick, A.; Shen, Y.; Tuchband, M.R.; Korblova, E.; Bedrov, D.; Walba, D.M.; Glaser, M.A.; et al. Chiral heliconical ground state of nanoscale pitch in a nematic liquid crystal of achiral molecular dimers. *Proc. Natl. Acad. Sci. USA* **2013**, *110*, 15931–15936. [[CrossRef](#)]
12. Chen, D.; Nakata, M.; Shao, R.; Tuchband, M.R.; Shuai, M.; Baumeister, U.; Weissflog, W.; Walba, D.M.; Glaser, M.A.; Maclennan, J.E.; et al. Twist-bend heliconical chiral nematic liquid crystal phase of an achiral rigid bent-core mesogen. *Phys. Rev. E Stat. Nonlinear Biol. Soft Matter Phys.* **2014**, *89*, 022506. [[CrossRef](#)]
13. Wang, Y.; Singh, G.; Agra-Kooijman, D.M.; Gao, M.; Bisoyi, H.K.; Xue, C.M.; Fisch, M.R.; Kumar, S.; Li, Q. Room temperature heliconical twist-bend nematic liquid crystal. *CryStengComm* **2015**, *17*, 2778–2782. [[CrossRef](#)]

14. Beguin, L.; Emsley, J.W.; Lelli, M.; Lesage, A.; Luckhurst, G.R.; Timimi, B.A.; Zimmermann, H. The chirality of a twist-bend nematic phase identified by nmr spectroscopy. *J. Phys. Chem. B* **2012**, *116*, 7940–7951. [[CrossRef](#)]
15. Meyer, C.; Luckhurst, G.R.; Dozov, I. Flexoelectrically driven electroclinic effect in the twist-bend nematic phase of achiral molecules with bent shapes. *Phys. Rev. Lett.* **2013**, *111*, 067801. [[CrossRef](#)]
16. Zhu, C.; Tuchband, M.R.; Young, A.; Shuai, M.; Scarbrough, A.; Walba, D.M.; Maclennan, J.E.; Wang, C.; Hexemer, A.; Clark, N.A. Resonant carbon k-edge soft x-ray scattering from lattice-free heliconical molecular ordering: Soft dilative elasticity of the twist-bend liquid crystal phase. *Phys. Rev. Lett.* **2016**, *116*, 147803. [[CrossRef](#)]
17. Stevenson, W.D.; Ahmed, Z.; Zeng, X.B.; Welch, C.; Ungar, G.; Mehl, G.H. Molecular organization in the twist-bend nematic phase by resonant x-ray scattering at the se k-edge and by saxs, waxes and gixrd. *Phys. Chem. Chem. Phys.* **2017**, *19*, 13449–13454. [[CrossRef](#)]
18. Samulski, E.T.; Vanakaras, A.G.; Photinos, D.J. The twist bend nematic: A case of mistaken identity. *Liq. Cryst.* **2020**, *47*, 2092–2097. [[CrossRef](#)]
19. Jokisaari, J.P.; Luckhurst, G.R.; Timimi, B.A.; Zhu, J.F.; Zimmermann, H. Twist-bend nematic phase of the liquid crystal dimer cb7cb: Orientational order and conical angle determined by xe-129 and h-2 nmr spectroscopy. *Liq. Cryst.* **2015**, *42*, 708–721.
20. Meyer, C.; Luckhurst, G.R.; Dozov, I. The temperature dependence of the heliconical tilt angle in the twist-bend nematic phase of the odd dimer cb7cb. *J. Mater. Chem. C* **2015**, *3*, 318–328. [[CrossRef](#)]
21. Singh, G.; Fu, J.X.; Agra-Kooijman, D.M.; Song, J.K.; Vengatesan, M.R.; Srinivasarao, M.; Fisch, M.R.; Kumar, S. X-ray and raman scattering study of orientational order in nematic and heliconical nematic liquid crystals. *Phys. Rev. E* **2016**, *94*, 060701. [[CrossRef](#)] [[PubMed](#)]
22. Zhang, Z.P.; Panov, V.P.; Nagaraj, M.; Mandle, R.J.; Goodby, J.W.; Luckhurst, G.R.; Jones, J.C.; Gleeson, H.F. Raman scattering studies of order parameters in liquid crystalline dimers exhibiting the nematic and twist-bend nematic phases. *J. Mater. Chem. C* **2015**, *3*, 10007–10016. [[CrossRef](#)]
23. Barnes, P.J.; Douglass, A.G.; Heeks, S.K.; Luckhurst, G.R. An enhanced odd even effect of liquid-crystal dimers orientational order in the alpha,omega-bis(4'-cyanobiphenyl-4-yl)alkanes. *Liq. Cryst.* **1993**, *13*, 603–613. [[CrossRef](#)]
24. Gorecka, E.; Vaupotic, N.; Zep, A.; Pocięcha, D.; Yoshioka, J.; Yamamoto, J.; Takezoe, H. A twist-bend nematic (n-tb) phase of chiral materials. *Angew. Chem. Int. Ed.* **2015**, *54*, 10155–10159. [[CrossRef](#)]
25. Tripathi, C.S.P.; Losada-Perez, P.; Glorieux, C.; Kohlmeier, A.; Tamba, M.G.; Mehl, G.H.; Leys, J. Nematic-nematic phase transition in the liquid crystal dimer cbc9cb and its mixtures with 5cb: A high-resolution adiabatic scanning calorimetric study. *Phys. Rev. E* **2011**, *84*, 041707. [[CrossRef](#)]
26. Mandle, R.J.; Davis, E.J.; Archbold, C.T.; Cowling, S.J.; Goodby, J.W. Microscopy studies of the nematic N_{TB} phase of 1,11-di-(1''-cyanobiphenyl-4-yl)undecane. *J. Mater. Chem. C* **2014**, *2*, 556–566. [[CrossRef](#)]
27. Robles-Hernandez, B.; Sebastian, N.; de la Fuente, M.R.; Lopez, D.O.; Diez-Berart, S.; Salud, J.; Ros, M.B.; Dunmur, D.A.; Luckhurst, G.R.; Timimi, B.A. Twist, tilt, and orientational order at the nematic to twist-bend nematic phase transition of 1'',9''-bis(4-cyanobiphenyl-4'-yl) nonane: A dielectric, h-2 nmr, and calorimetric study. *Phys. Rev. E* **2015**, *92*, 062505. [[CrossRef](#)]
28. Sebastian, N.; Lopez, D.O.; Robles-Hernandez, B.; de la Fuente, M.R.; Salud, J.; Perez-Jubindo, M.A.; Dunmur, D.A.; Luckhurst, G.R.; Jackson, D.J. Dielectric, calorimetric and mesophase properties of 1''-(2',4-difluorobiphenyl-4'-yloxy)-9''-(4-cyanobiphenyl-4'-yloxy) nonane: An odd liquid crystal dimer with a monotropic mesophase having the characteristics of a twist-bend nematic phase. *Phys. Chem. Chem. Phys.* **2014**, *16*, 21391–21406. [[CrossRef](#)]
29. Adlem, K.; Copic, M.; Luckhurst, G.R.; Mertelj, A.; Parri, O.; Richardson, R.M.; Snow, B.D.; Timimi, B.A.; Tuffin, R.P.; Wilkes, D. Chemically induced twist-bend nematic liquid crystals, liquid crystal dimers, and negative elastic constants. *Phys. Rev. E Stat. Nonlinear Biol. Soft Matter Phys.* **2013**, *88*, 022503. [[CrossRef](#)]
30. Ribeiro de Almeida, R.R.; Zhang, C.; Parri, O.; Sprunt, S.N.; Jáklí, A. Nanostructure and dielectric properties of a twist-bend nematic liquid crystal mixture. *Liq. Cryst.* **2014**, *41*, 1661–1667. [[CrossRef](#)]
31. Salili, S.M.; Kim, C.; Sprunt, S.; Gleeson, J.T.; Parri, O.; Jakli, A. Flow properties of a twist-bend nematic liquid crystal. *RSC Adv.* **2014**, *4*, 57419–57423. [[CrossRef](#)]
32. Mandle, R.J. The dependency of twist-bend nematic liquid crystals on molecular structure: A progression from dimers to trimers, oligomers and polymers. *Soft Matter* **2016**, *12*, 7883–7901. [[CrossRef](#)] [[PubMed](#)]
33. Imrie, C.T.; Henderson, P.A. Liquid crystal dimers and oligomers. *Curr. Opin. Colloid Interface Sci.* **2002**, *7*, 298–311. [[CrossRef](#)]
34. Reddy, R.A.; Tschierske, C. Bent-core liquid crystals: Polar order, superstructural chirality and spontaneous desymmetrisation in soft matter systems. *J. Mater. Chem.* **2006**, *16*, 907–961. [[CrossRef](#)]
35. Henderson, P.A.; Seddon, J.M.; Imrie, C.T. Methylene- and ether-linked liquid crystal dimers ii. Effects of mesogenic linking unit and terminal chain length. *Liq. Cryst.* **2005**, *32*, 1499–1513. [[CrossRef](#)]
36. Ramou, E.; Welch, C.; Hussey, J.; Ahmed, Z.; Karahaliou, P.K.; Mehl, G.H. The induction of the N_{tb} phase in mixtures. *Liq. Cryst.* **2018**, *45*, 1929–1935. [[CrossRef](#)]
37. Emsley, J.W.; Luckhurst, G.R.; Shilstone, G.N. The orientational order of nematogenic molecules with a flexible core—A dramatic odd even effect. *Mol. Phys.* **1984**, *53*, 1023–1028. [[CrossRef](#)]
38. Emsley, J.W.; Luckhurst, G.R.; Shilstone, G.N.; Sage, I. The preparation and properties of the alpha,omega-bis(4,4'-cyanobiphenyloxy)alkanes—Nematogenic molecules with a flexible core. *Mol. Cryst. Liq. Cryst.* **1984**, *102*, 223–233. [[CrossRef](#)]

39. Panov, V.P.; Vij, J.K.; Mehl, G.H. Twist-bend nematic phase in cyanobiphenyls and difluoroterphenyls bimesogens. *Liq. Cryst.* **2017**, *44*, 147–159.
40. Miglioli, I.; Bacchicchi, C.; Arcioni, A.; Kohlmeier, A.; Mehl, G.H.; Zannoni, C. Director configuration in the twist-bend nematic phase of cb11cb. *J. Mater. Chem. C* **2016**, *4*, 9887–9896. [[CrossRef](#)]
41. Yu, G.; Wilson, M.R. All-atom simulations of bent liquid crystal dimers: The twist-bend nematic phase and insights into conformational chirality. *Soft Matter* **2022**, *18*, 3087–3096. [[CrossRef](#)] [[PubMed](#)]
42. Mandle, R.J.; Goodby, J.W. Order parameters, orientational distribution functions and heliconical tilt angles of oligomeric liquid crystals. *Phys. Chem. Chem. Phys.* **2019**, *21*, 6839–6843. [[CrossRef](#)] [[PubMed](#)]
43. Heist, L.M.; Samulski, E.T.; Welch, C.; Ahmed, Z.; Mehl, G.H.; Vanakaras, A.G.; Photinos, D.J. Probing molecular ordering in the nematic phases of para-linked bimesogen dimers through nmr studies of flexible prochiral solutes. *Liq. Cryst.* **2020**, *47*, 2058–2073. [[CrossRef](#)]
44. Mandle, R.J.; Davis, E.J.; Voll, C.C.A.; Archbold, C.T.; Goodby, J.W.; Cowling, S.J. The relationship between molecular structure and the incidence of the N_{TB} phase. *Liq. Cryst.* **2015**, *42*, 688–703.
45. Mandle, R.J.; Davis, E.J.; Archbold, C.T.; Voll, C.C.; Andrews, J.L.; Cowling, S.J.; Goodby, J.W. Apolar bimesogens and the incidence of the twist-bend nematic phase. *Chem. Eur. J.* **2015**, *21*, 8158–8167. [[CrossRef](#)]
46. Salamończyk, M.; Mandle, R.J.; Makal, A.; Liebman-Peláez, A.; Feng, J.; Goodby, J.W.; Zhu, C. Double helical structure of the twist-bend nematic phase investigated by resonant x-ray scattering at the carbon and sulfur k-edges. *Soft Matter* **2018**, *14*, 9760–9763. [[CrossRef](#)]
47. Mandle, R.J.; Goodby, J.W. Progression from nano to macro science in soft matter systems: Dimers to trimers and oligomers in twist-bend liquid crystals. *RSC Adv.* **2016**, *6*, 34885–34893. [[CrossRef](#)]
48. Mandle, R.J.; Goodby, J.W. Does topology dictate the incidence of the twist-bend phase? Insights gained from novel unsymmetrical bimesogens. *Chem.—A Eur. J.* **2016**, *22*, 18456–18464. [[CrossRef](#)]
49. Hird, M. Fluorinated liquid crystals—Properties and applications. *Chem. Soc. Rev.* **2007**, *36*, 2070–2095. [[CrossRef](#)]
50. Sepelj, M.; Lesac, A.; Baumeister, U.; Diele, S.; Bruce, D.W.; Hamersak, Z. Dimeric salicylaldehyde-based mesogens with flexible spacers: Parity-dependent mesomorphism. *Chem. Mater.* **2006**, *18*, 2050–2058. [[CrossRef](#)]
51. Ivsic, T.; Vinkovic, M.; Baumeister, U.; Mikleusevic, A.; Lesac, A. Retraction. Milestone in the N_{TB} phase investigation and beyond: Direct insight into molecular self-assembly. *Soft Matter* **2015**, *11*, 6716. [[CrossRef](#)] [[PubMed](#)]
52. Ivsic, T.; Vinkovic, M.; Baumeister, U.; Mikleusevic, A.; Lesac, A. Towards understanding the N_{TB} phase: A combined experimental, computational and spectroscopic study. *RSC Adv.* **2016**, *6*, 5000–5007. [[CrossRef](#)]
53. Sepelj, M.; Lesac, A.; Baumeister, U.; Diele, S.; Nguyen, H.L.; Bruce, D.W. Intercalated liquid-crystalline phases formed by symmetric dimers with an alpha,omega-diiminoalkylene spacer. *J. Mater. Chem.* **2007**, *17*, 1154–1165. [[CrossRef](#)]
54. Archbold, C.T.; Mandle, R.J.; Andrews, J.L.; Cowling, S.J.; Goodby, J.W. Conformational landscapes of bimesogenic compounds and their implications for the formation of modulated nematic phases. *Liq. Cryst.* **2017**, *44*, 2079–2088. [[CrossRef](#)]
55. Mandle, R.J.; Archbold, C.T.; Sarju, J.P.; Andrews, J.L.; Goodby, J.W. The dependency of nematic and twist-bend mesophase formation on bend angle. *Sci. Rep.* **2016**, *6*, 36682. [[CrossRef](#)]
56. Mandle, R.J.; Goodby, J.W. Molecular flexibility and bend in semi-rigid liquid crystals: Implications for the heliconical nematic ground state. *Chem.—A Eur. J.* **2019**, *25*, 14454–14459. [[CrossRef](#)]
57. Arakawa, Y.; Komatsu, K.; Tsuji, H. Twist-bend nematic liquid crystals based on thioether linkage. *New J. Chem.* **2019**, *43*, 6786–6793. [[CrossRef](#)]
58. Arakawa, Y.; Tsuji, H. Selenium-linked liquid crystal dimers for twist-bend nematogens. *J. Mol. Liq.* **2019**, *289*, 111097. [[CrossRef](#)]
59. Paterson, D.A.; Gao, M.; Kim, Y.K.; Jamali, A.; Finley, K.L.; Robles-Hernandez, B.; Diez-Berart, S.; Salud, J.; de la Fuente, M.R.; Timimi, B.A.; et al. Understanding the twist-bend nematic phase: The characterisation of 1-(4-cyanobiphenyl-4'-yloxy)-6-(4-cyanobiphenyl-4'-yl)hexane (CB6OCB) and comparison with CB7CB. *Soft Matter* **2016**, *12*, 6827–6840. [[CrossRef](#)]
60. Paterson, D.A.; Abberley, J.P.; Harrison, W.T.A.; Storey, J.M.D.; Imrie, C.T. Cyanobiphenyl-based liquid crystal dimers and the twist-bend nematic phase. *Liq. Cryst.* **2017**, *44*, 127–146. [[CrossRef](#)]
61. Arakawa, Y.; Komatsu, K.; Shiba, T.; Tsuji, H. Methylene- and thioether-linked cyanobiphenyl-based liquid crystal dimers cbnscb exhibiting room temperature twist-bend nematic phases and glasses. *Mater. Adv.* **2021**, *2*, 1760–1773. [[CrossRef](#)]
62. Tuchband, M.R.; Paterson, D.A.; Salamończyk, M.; Norman, V.A.; Scarbrough, A.N.; Forsyth, E.; Garcia, E.; Wang, C.; Storey, J.M.D.; Walba, D.M.; et al. Distinct differences in the nanoscale behaviors of the twist-bend liquid crystal phase of a flexible linear trimer and homologous dimer. *Proc. Natl. Acad. Sci. USA* **2019**, *116*, 10698–10704. [[CrossRef](#)] [[PubMed](#)]
63. Cao, Y.; Feng, J.; Nallapaneni, A.; Arakawa, Y.; Zhao, K.; Zhang, H.; Mehl, G.H.; Zhu, C.; Liu, F. Deciphering helix assembly in the heliconical nematic phase via tender resonant x-ray scattering. *J. Mater. Chem. C* **2021**, *9*, 10020–10028. [[CrossRef](#)]
64. Cruickshank, E.; Salamończyk, M.; Pocięcha, D.; Strachan, G.J.; Storey, J.M.D.; Wang, C.; Feng, J.; Zhu, C.; Gorecka, E.; Imrie, C.T. Sulfur-linked cyanobiphenyl-based liquid crystal dimers and the twist-bend nematic phase. *Liq. Cryst.* **2019**, *46*, 1595–1609. [[CrossRef](#)]
65. Arakawa, Y.; Komatsu, K.; Ishida, Y.; Igawa, K.; Tsuji, H. Carbonyl- and thioether-linked cyanobiphenyl-based liquid crystal dimers exhibiting twist-bend nematic phases. *Tetrahedron* **2021**, *81*, 131870. [[CrossRef](#)]
66. Archbold, C.T.; Davis, E.J.; Mandle, R.J.; Cowling, S.J.; Goodby, J.W. Chiral dopants and the twist-bend nematic phase—induction of novel mesomorphic behaviour in an apolar bimesogen. *Soft Matter* **2015**, *11*, 7547–7557. [[CrossRef](#)]

67. Zep, A.; Aya, S.; Aihara, K.; Ema, K.; Pocięcha, D.; Madrak, K.; Bernatowicz, P.; Takezoe, H.; Gorecka, E. Multiple nematic phases observed in chiral mesogenic dimers. *J. Mater. Chem. C* **2013**, *1*, 46–49. [[CrossRef](#)]
68. Salamończyk, M.; Vaupotič, N.; Pocięcha, D.; Wang, C.; Zhu, C.; Gorecka, E. Structure of nanoscale-pitch helical phases: Blue phase and twist-bend nematic phase resolved by resonant soft x-ray scattering. *Soft Matter* **2017**, *13*, 6694–6699. [[CrossRef](#)]
69. Paterson, D.A.; Xiang, J.; Singh, G.; Walker, R.; Agra-Kooijman, D.M.; Martínez-Felipe, A.; Gao, M.; Storey, J.M.D.; Kumar, S.; Lavrentovich, O.D.; et al. Reversible isothermal twist–bend nematic–nematic phase transition driven by the photoisomerization of an azobenzene-based nonsymmetric liquid crystal dimer. *J. Am. Chem. Soc.* **2016**, *138*, 5283–5289. [[CrossRef](#)]
70. Mandle, R.J.; Davis, E.J.; Lobato, S.A.; Vol, C.C.A.; Cowling, S.J.; Goodby, J.W. Synthesis and characterisation of an unsymmetrical, ether-linked, fluorinated bimesogen exhibiting a new polymorphism containing the N_{TB} or ‘twist-bend’ phase. *Phys. Chem. Chem. Phys.* **2014**, *16*, 6907–6915. [[CrossRef](#)]
71. Walker, R.; Pocięcha, D.; Storey, J.M.D.; Gorecka, E.; Imrie, C.T. The chiral twist-bend nematic phase (N^*_{TB}). *Chem.–A Eur. J.* **2019**, *25*, 13329–13335. [[CrossRef](#)] [[PubMed](#)]
72. Meyer, C. Nematic twist-bend phase under external constraints. *Liq. Cryst.* **2016**, *43*, 2144–2162. [[CrossRef](#)]
73. Schroder, M.W.; Diele, S.; Pelzl, G.; Dunemann, U.; Kresse, H.; Weissflog, W. Different nematic phases and a switchable smcp phase formed by homologues of a new class of asymmetric bent-core mesogens. *J. Mater. Chem.* **2003**, *13*, 1877–1882. [[CrossRef](#)]
74. Tamba, M.G.; Baumeister, U.; Pelzl, G.; Weissflog, W. Banana-calamitic dimers: Further variations of the bent-core mesogenic unit. *Ferroelectrics* **2014**, *468*, 52–76. [[CrossRef](#)]
75. Gortz, V.; Southern, C.; Roberts, N.W.; Gleeson, H.F.; Goodby, J.W. Unusual properties of a bent-core liquid-crystalline fluid. *Soft Matter* **2009**, *5*, 463–471. [[CrossRef](#)]
76. Yoshizawa, A. Unconventional liquid crystal oligomers with a hierarchical structure. *J. Mater. Chem.* **2008**, *18*, 2877–2889. [[CrossRef](#)]
77. Keller, P. Synthesis of new mesomorphic polyesters by polymerization of bifunctional monomers. *Mol. Cryst. Liq. Cryst.* **1985**, *123*, 247–256. [[CrossRef](#)]
78. Imrie, C.T.; Luckhurst, G.R. Liquid crystal trimers. The synthesis and characterisation of the 4,4′-bis[ω-(4-cyanobiphenyl-4′-yloxy)alkoxy]biphenyls. *J. Mater. Chem.* **1998**, *8*, 1339–1343. [[CrossRef](#)]
79. Andersch, J.; Diele, S.; Lose, D.; Tschierske, C. Synthesis and liquid crystalline properties of novel laterally connected trimesogens and tetramesogens. *Liq. Cryst.* **1996**, *21*, 103–113. [[CrossRef](#)]
80. Kreuder, W.; Ringsdorf, H.; Herrmannschonherr, O.; Wendorff, J.H. The wheel of mainz as a liquid-crystal—Structural variation and mesophase properties of trimeric discotic compounds. *Angew. Chem.-Int. Ed. Engl.* **1987**, *26*, 1249–1252. [[CrossRef](#)]
81. Griffin, A.C.; Sullivan, S.L.; Hughes, W.E. Effect of molecular structure on mesomorphism xxi. Monodisperse tetrameric model compounds for liquid crystalline polymers. *Liq. Cryst.* **1989**, *4*, 677–684. [[CrossRef](#)]
82. Imrie, C.T.; Stewart, D.; Remy, C.; Christie, D.W.; Hamley, I.W.; Harding, R. Liquid crystal tetramers. *J. Mater. Chem.* **1999**, *9*, 2321–2325. [[CrossRef](#)]
83. Yelamaggad, C.V.; Nagamani, S.A.; Hiremath, U.S.; Rao, D.S.S.; Prasad, S.K. The first examples of monodisperse liquid crystalline tetramers possessing four non-identical anisometric segments. *Liq. Cryst.* **2002**, *29*, 231–236. [[CrossRef](#)]
84. Henderson, P.A.; Imrie, C.T. Semiflexible liquid crystalline tetramers as models of structurally analogous copolymers. *Macromolecules* **2005**, *38*, 3307–3311. [[CrossRef](#)]
85. Yelamaggad, C.V.; Achalkumar, A.S.; Rao, D.S.S.; Prasad, S.K. Monodisperse linear supermolecules stabilizing unusual fluid layered phases. *Org. Lett.* **2007**, *9*, 2641–2644. [[CrossRef](#)]
86. Jansze, S.M.; Martínez-Felipe, A.; Storey, J.M.; Marcelis, A.T.; Imrie, C.T. A twist-bend nematic phase driven by hydrogen bonding. *Angew. Chem. Int. Ed. Engl.* **2015**, *54*, 643–646. [[CrossRef](#)]
87. Martínez-Felipe, A.; Imrie, C.T. The role of hydrogen bonding in the phase behaviour of supramolecular liquid crystal dimers. *J. Mol. Struct.* **2015**, *1100*, 429–437. [[CrossRef](#)]
88. Paterson, D.A.; Martínez-Felipe, A.; Jansze, S.M.; Marcelis, A.T.M.; Storey, J.M.D.; Imrie, C.T. New insights into the liquid crystal behaviour of hydrogen-bonded mixtures provided by temperature-dependent ftir spectroscopy. *Liq. Cryst.* **2015**, *42*, 928–939. [[CrossRef](#)]
89. Wang, Y.; Yoon, H.G.; Bisoyi, H.K.; Kumar, S.; Li, Q. Hybrid rod-like and bent-core liquid crystal dimers exhibiting biaxial smectic a and nematic phases. *J. Mater. Chem.* **2012**, *22*, 20363–20367. [[CrossRef](#)]
90. Mandle, R.J.; Goodby, J.W. A liquid crystalline oligomer exhibiting nematic and twist-bend nematic mesophases. *Chemphyschem* **2016**, *17*, 967–970. [[CrossRef](#)]
91. Mandle, R.J.; Goodby, J.W. A nanohelicoidal nematic liquid crystal formed by a non-linear duplexed hexamer. *Angew. Chem. Int. Ed. Engl.* **2018**, *57*, 7096–7100. [[CrossRef](#)] [[PubMed](#)]
92. Saha, R.; Babakhanova, G.; Parsouzi, Z.; Rajabi, M.; Gyawali, P.; Welch, C.; Mehl, G.H.; Gleeson, J.; Lavrentovich, O.D.; Sprunt, S.; et al. Oligomeric odd–even effect in liquid crystals. *Mater. Horiz.* **2019**, *6*, 1905–1912. [[CrossRef](#)]
93. Panov, V.P.; Nagaraj, M.; Vij, J.K.; Panarin, Y.P.; Kohlmeier, A.; Tamba, M.G.; Lewis, R.A.; Mehl, G.H. Spontaneous periodic deformations in nonchiral planar-aligned bimesogens with a nematic–nematic transition and a negative elastic constant. *Phys. Rev. Lett.* **2010**, *105*, 167801. [[CrossRef](#)] [[PubMed](#)]
94. Panov, V.P.; Balachandran, R.; Nagaraj, M.; Vij, J.K.; Tamba, M.G.; Kohlmeier, A.; Mehl, G.H. Microsecond linear optical response in the unusual nematic phase of achiral bimesogens. *Appl. Phys. Lett.* **2011**, *99*, 261903. [[CrossRef](#)]

95. Sebastian, N.; Tamba, M.G.; Stannarius, R.; de la Fuente, M.R.; Salamonczyk, M.; Cukrov, G.; Gleeson, J.; Sprunt, S.; Jakli, A.; Welch, C.; et al. Mesophase structure and behaviour in bulk and restricted geometry of a dimeric compound exhibiting a nematic-nematic transition. *Phys. Chem. Chem. Phys.* **2016**, *18*, 19299–19308. [[CrossRef](#)] [[PubMed](#)]
96. Merkel, K.; Loska, B.; Welch, C.; Mehl, G.H.; Kocot, A. The role of intermolecular interactions in stabilizing the structure of the nematic twist-bend phase. *RSC Adv.* **2021**, *11*, 2917–2925. [[CrossRef](#)] [[PubMed](#)]
97. Cukrov, G.; Mosaddeghian Golestani, Y.; Xiang, J.; Nastishin, Y.A.; Ahmed, Z.; Welch, C.; Mehl, G.H.; Lavrentovich, O.D. Comparative analysis of anisotropic material properties of uniaxial nematics formed by flexible dimers and rod-like monomers. *Liq. Cryst.* **2017**, *44*, 219–231. [[CrossRef](#)]
98. Saha, R.; Feng, C.; Welch, C.; Mehl, G.H.; Feng, J.; Zhu, C.; Gleeson, J.; Sprunt, S.; Jakli, A. The interplay between spatial and heliconical orientational order in twist-bend nematic materials. *Phys. Chem. Chem. Phys.* **2021**, *23*, 4055–4063. [[CrossRef](#)]
99. Arakawa, Y.; Komatsu, K.; Shiba, T.; Tsuji, H. Phase behaviors of classic liquid crystal dimers and trimers: Alternate induction of smectic and twist-bend nematic phases depending on spacer parity for liquid crystal trimers. *J. Mol. Liq.* **2021**, *326*, 115319. [[CrossRef](#)]
100. Arakawa, Y.; Komatsu, K.; Ishida, Y.; Shiba, T.; Tsuji, H. Thioether-linked liquid crystal trimers: Odd–even effects of spacers and the influence of thioether bonds on phase behavior. *Materials* **2022**, *15*, 1709. [[CrossRef](#)]
101. Al-Janabi, A.; Mandle, R.J. Utilising saturated hydrocarbon isosteres of para benzene in the design of twist-bend nematic liquid crystals. *ChemPhysChem* **2020**, *21*, 697–701. [[CrossRef](#)] [[PubMed](#)]
102. Majewska, M.M.; Forsyth, E.; Pocięcha, D.; Wang, C.; Storey, J.M.D.; Imrie, C.T.; Gorecka, E. Controlling spontaneous chirality in achiral materials: Liquid crystal oligomers and the heliconical twist-bend nematic phase. *Chem. Commun.* **2022**. [[CrossRef](#)] [[PubMed](#)]
103. Walker, R.; Pocięcha, D.; Abberley, J.P.; Martinez-Felipe, A.; Paterson, D.A.; Forsyth, E.; Lawrence, G.B.; Henderson, P.A.; Storey, J.M.D.; Gorecka, E.; et al. Spontaneous chirality through mixing achiral components: A twist-bend nematic phase driven by hydrogen-bonding between unlike components. *Chem. Commun.* **2018**, *54*, 3383–3386. [[CrossRef](#)] [[PubMed](#)]
104. Abberley, J.P.; Killah, R.; Walker, R.; Storey, J.M.D.; Imrie, C.T.; Salamończyk, M.; Zhu, C.; Gorecka, E.; Pocięcha, D. Heliconical smectic phases formed by achiral molecules. *Nat. Commun.* **2018**, *9*, 228. [[CrossRef](#)]
105. Walker, R.; Pocięcha, D.; Salamończyk, M.; Storey, J.M.D.; Gorecka, E.; Imrie, C.T. Supramolecular liquid crystals exhibiting a chiral twist-bend nematic phase. *Mater. Adv.* **2020**, *1*, 1622–1630. [[CrossRef](#)]
106. Walker, R.; Pocięcha, D.; Martinez-Felipe, A.; Storey, J.M.; Gorecka, E.; Imrie, C.T. Twist-bend nematogenic supramolecular dimers and trimers formed by hydrogen bonding. *Crystals* **2020**, *10*, 175. [[CrossRef](#)]
107. Nguyen, H.L.; Horton, P.N.; Hursthouse, M.B.; Legon, A.C.; Bruce, D.W. Halogen bonding: A new interaction for liquid crystal formation. *J. Am. Chem. Soc.* **2004**, *126*, 16–17. [[CrossRef](#)]